AICS TECHNICAL REPORT
NO. 2016-001

A SIMPLE METHOD FOR DETECTING THE LIFECYCLE OF DEEP MOIST CONVECTION FROM DISCRETIZED DATA

By

YOSHIAKI MIYAMOTO[1,2], TSUYOSHI YAMAURA[2], RYUJI YOSHIDA[2], HISASHI YASHIRO[2], HIROFUMI TOMITA[2,3], AND YOSHIYUKI KAJIKAWA[2]

[1] ROSENSTIEL SCHOOL OF MARINE AND ATMOSPHERIC SCIENCE, THE UNIVERSITY OF MIAMI
[2] RIKEN ADVANCED INSTITUTE FOR COMPUTATIONAL SCIENCE
[3] SEAMLESS ENVIRONMENTAL PREDICTION RESEARCH, JAPAN AGENCY FOR MARINE EARTH SCIENCE AND TECHNOLOGY

SUBMITTED ON 05/04/2016
ACCEPTED ON 08/07/2016

Published and copyrighted by
RIKEN Advanced Institute for Computational Science (AICS)
7-1-26 Minatojima-minami-machi, Chuo-ku, Kobe, 650-0047, Japan

A simple method for detecting the lifecycle of deep moist convection from discretized data

Yoshiaki Miyamoto[1,2], Tsuyoshi Yamaura[2], Ryuji Yoshida[2],
Hisashi Yashiro[2], Hirofumi Tomita[2,3], and Yoshiyuki Kajikawa[2]

1: Rosenstiel School of Marine and Atmospheric Science, The University of Miami

2: RIKEN Advanced Institute for Computational Science

3: Seamless Environmental Prediction Research, Japan Agency for Marine–Earth Science and Technology

Abstract

Deep moist convection plays a crucial role in transporting energy and momentum in the Earth's atmosphere. Examining the convection is fundamentally important for better understanding of various atmospheric phenomena, e.g., typhoons, as well as the convection itself. We developed a simple methodology for detecting the lifecycle of convection from discrete spatiotemporal data such as output of model simulations or reanalyses, which are often used in the Atmospheric Science research. The method includes only a few thresholds and hence it can be applied to data of global atmosphere in which environmental conditions for the convection are largely different in space and time. We tested and verified the method on a global simulation with high spatiotemporal resolution.

1 Introduction

The Earth's atmosphere is characterized by rotational motion and stratification due to gravity, and the majority of flow motion is well approximated as being horizontally two–dimensional. However, convection plays a key role in vertically transporting energy in the atmosphere. Convection is active in the troposphere where there is a near balance between heating due to solar radiation, re-radiation from the atmosphere itself, and vertical transport of heat by convection.

A defining characteristic of the Earth ' s atmosphere is the large abundance of water present. In the range of pressures and temperatures found in the atmosphere, water can change its phase (e.g., Houze 1993, Emanuel 1993). Consider an air parcel that contains a certain mass of dry air and a certain amount of water vapor. As this air parcel is lifted

upwards, the pressure and temperature of the parcel decrease. If the mixing ratio of water vapor in the parcel exceeds the saturation mixing ratio (which decreases with decreasing temperature), the vapor condenses, changing from gas to liquid. If the air parcel continues moving upward and passes the 0–deg temperature level, the water will change its phase to ice. This condensation heats the air surrounding the water droplet due to the vapor ' s decrease in molecular kinetic energy. Hence, the following positive feedback may occur. The heated air parcel will tend to be less dense than the surrounding air (i.e., it will be positively buoyant). This positive buoyancy causes the air parcel to move upward more quickly, allowing a larger amount of water to condense. This condensation then further increases the temperature of the air parcel. This positive feedback process can continue until the air parcel is no longer positively buoyant. The strongest convection can reach altitudes of 10 – 15 km because of this positive feedback process. It should be noted that we have neglected the presence of rain, which would tend to accelerate the vertical motion and remove water mass from the air parcel.

Convection transports mass and energy in the vertical direction (e.g., LeMone et al. 1984, Tung and Yanai 2002a,b). Synoptic scale atmospheric motion is characterized by two horizontal dimensions, but even in that case, convection plays a fundamental role in transporting physical quantities in the vertical direction. The troposphere, which is the lower–most layer in the atmosphere extending from the ground up to altitudes of approximately 10–15 km, is characterized by continuous convective heating and radiative cooling (Manabe and Strickler 1964, Manabe and Wetherald 1967). At any given moment, the atmosphere contains a number of convective cells spanning the entire vertical extent of the troposphere with water in liquid and/or ice phases.

Figure **??** depicts a schematic view of the lifecycle of deep moist convection (cf. Byers and Braham 1948). Condensation occurs in the updraft region as a result of low-level air converging in the early development phase. In the mature stage, liquid and solid water phases are present in the entire troposphere and strong updrafts and downdrafts co-exist within a single convection cell. Thereafter, the downdraft produced by precipitation dominates, and the convection decays. The typical timescale from genesis to dissipation is 20–30 minutes. Both inside and near the convection cell, the fluid motion is highly perturbed, which causes significant mixing at the outer edge of the convection cell (e.g., Dawe and Austin 2013). Whereas positive buoyancy due to condensation will tend to keep the convection cell narrow (Bjerknes 1938), this diffusion tends to expand the horizontal scale of the cloudy convective region.

Convection produces a large amount of precipitation throughout the phase-change process. Localized convection can sometimes be the source of local downpours, potentially leading to local disasters. The timescale for convection is short compared with the timescales of larger weather systems, such as mid-latitudinal lows or fronts. Additionally,

the physical process of convection is highly nonlinear; this is due mainly to the moist processes (phase change) and partly to the smallness of flow scale[1]. This makes forecasting convection difficult, and the accurate prediction of convection is necessary for disaster prevention.

Convection can be regarded as cloudy, organized disturbances such as the Madden-Julian oscillation, tropical cyclones (typhoons), or mid-latitudinal lows. Modeling studies (Miyamoto et al. 2015 and Kajikawa et al. 2016) used global simulations to show that convective features are remarkably different among these disturbances: the vertical extent of convection is higher in tropical disturbances such as the Madden-Julian oscillation or tropical cyclones, but the intensity (vertical velocity) is stronger in the Madden-Julian oscillation. These researchers concluded that convection intensity depends on whether the convection forms with or without strong flow forcing and background stability, whereas the vertical extent simply depends on latitudinal variations in static stability. Their conclusions indicate that the detailed effects of convection need to be properly accounted for to simulate or predict cloudy disturbances. In other words, more effort to comprehensively examine the differences among the disturbances is needed to better understand and more accurately predict cloudy disturbances that can cause local disasters.

Due to the importance of convection and the popularity of gridded (discretized) data, previous studies have proposed methodologies for detecting deep convection using discretized data sets. Dawe and Austion (2012) developed a technique for tracking cloud cells in the spatiotemporal dimension using very high-resolution data. This technique detects conditions ranging from dry phases (plumes)to moist shallow cumulus clouds. Plant (2009) proposed a sophisticated method for tracking clouds in model simulations; this method is also applicable to high-resolution data that resolves convection cores over multiple grid points. Additionally, both methods can capture cloud cell mergers and splitting events. Although these methods are useful and highly accurate, they require a number of steps to implement within numerical models or to apply to online model calculation programs.

In this report, we propose a simple method for extracting the lifecycle of convection from a data set that is discretized in spatiotemporal dimensions (such as data or results from numerical models). This method enables researchers to address the physics of convection using conventional data sets. The method developed here can be used to perform detailed statistical analyses of convection. Given the observed spatial scale of convection, the data grid spacing might need to be coarser than several hundred meters; beyond this the convection core can fluctuate in time in a single convection cell. This methodology has been used by Miyamoto et al. (2013, 2015) and Kajikawa et al. (2016).

[1]The nonlinear advection terms are large compared with the others.

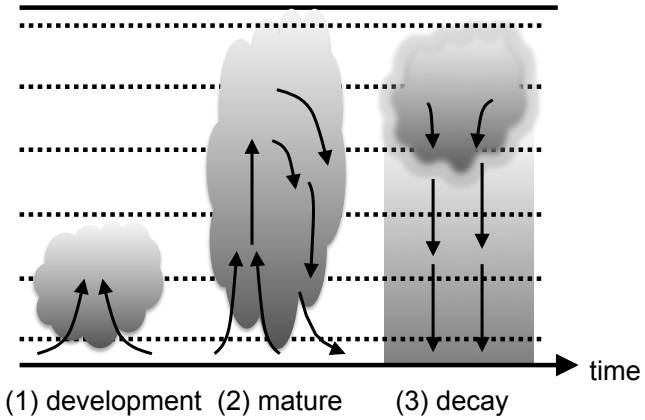

Figure 1: Schematic of the lifecycle of deep moist convection. The abscissa and ordinate are the horizontal and vertical directions, respectively. The topmost altitude of the panels approximately corresponds to the tropopause height. The shaded area represents a large amount of hydrometeors, while the gray blurred region in (3) represents the presence of rainfall. The yellow arrows indicate the flow direction. The left, center, and right panels respectively show the genesis/development, mature, and decay phase.

2 Proposed methodology of extracting the convection

The method proposed here mainly consists of two processes: (1) detecting the convection core grid points and (2) producing the lifecycle of convection. We first detect *convective* and *convection core* grid points by applying simple definitions at each time step. Then, the temporal connections between convection core grid points are diagnosed to determine the convection lifecycle.

2.1 Convective and convection core grid points

First, the atmosphere is vertically divided into Nz layers starting from the top of the boundary layer ($\sim$ 1 km) up to the tropopause. Here we have chosen $Nz = 5$; we conducted several sensitivity tests varying Nz, and we found that 5 appears to produce the most reasonable results. For this value of Nz, each layer has a depth of a few kilometers. Next, to identify *convective* grid points in each layer at every time step (cf. the gray points in Fig. **??**), we select grid points that satisfy the following conditions:

1. layer–averaged q_t is larger than 0.2 g kg^{-1}
2. layer–averaged w exceeds 0 m s^{-1},

where q_t is the total hydrometeors and w is the vertical velocity. The layer average represents the mean value in the layer (cf. Fig. **??**), and the averages are weighted by distance.

We then examine the following two conditions:

3. $\nabla_h w$ averaged inside and below the layer is larger than 0 s^{-1} in all directions
4. no neighboring grid points are convective grid points.

Girds satisfying all four conditions are defined as *convection*-core grid points (cf. the white point in Fig. **??**). Note here that $\nabla_h \equiv \partial/\partial x_i$ represents the horizontal differential in the x_i direction, where i is the number of grid points adjacent to the current grid point. At this point, the following information:

- horizontal grid points at which convection is detected,
- layer at which the convection is present, and
- time,

is stored as a convective grid point.

2.2 Lifecycle

We define the lifecycle of convection in discretized data as a time sequence of convection grid points in a certain area and time-range that are detected using the method above. The detected convection-core grid points are tracked in time using the following method to extract candidates for convection lifecycles. To determine whether convection core $C001_{t_a}$ (where '001' represents the ID of the convection core grid point) at $t = t_a$ is connected to core $C001_{t_a+\Delta t}$ at $t = t_a + \Delta t$ (where Δt is the temporal resolution of the data), we consider the following conditions:

1. $C001_{t_a+\Delta t}$ is located within Nx grid points of $C001_{t_a}$,
2. $C001_{t_a+\Delta t}$ is in the same layer or is one layer higher than $C001_{t_a}$, and
3. $C001_{t_a+\Delta t}$ has not yet been identified as the survivor of other cores at $t = t_a + \Delta t$.

After performing some sensitivity tests, we set $Nx = 2$, so grid points within two grid points of $C001_{t_a}$ are searched at the next time step $t_a + \Delta t$; this condition can be changed depending on the spatiotemporal resolution of the data set, as we discuss later.

Let us now consider that a candidate satisfying all the conditions ($C001_{t_a}$) is found. If it is a survivor of a core at $t = t_a - \Delta t$, the lifetime of that core is increased by one

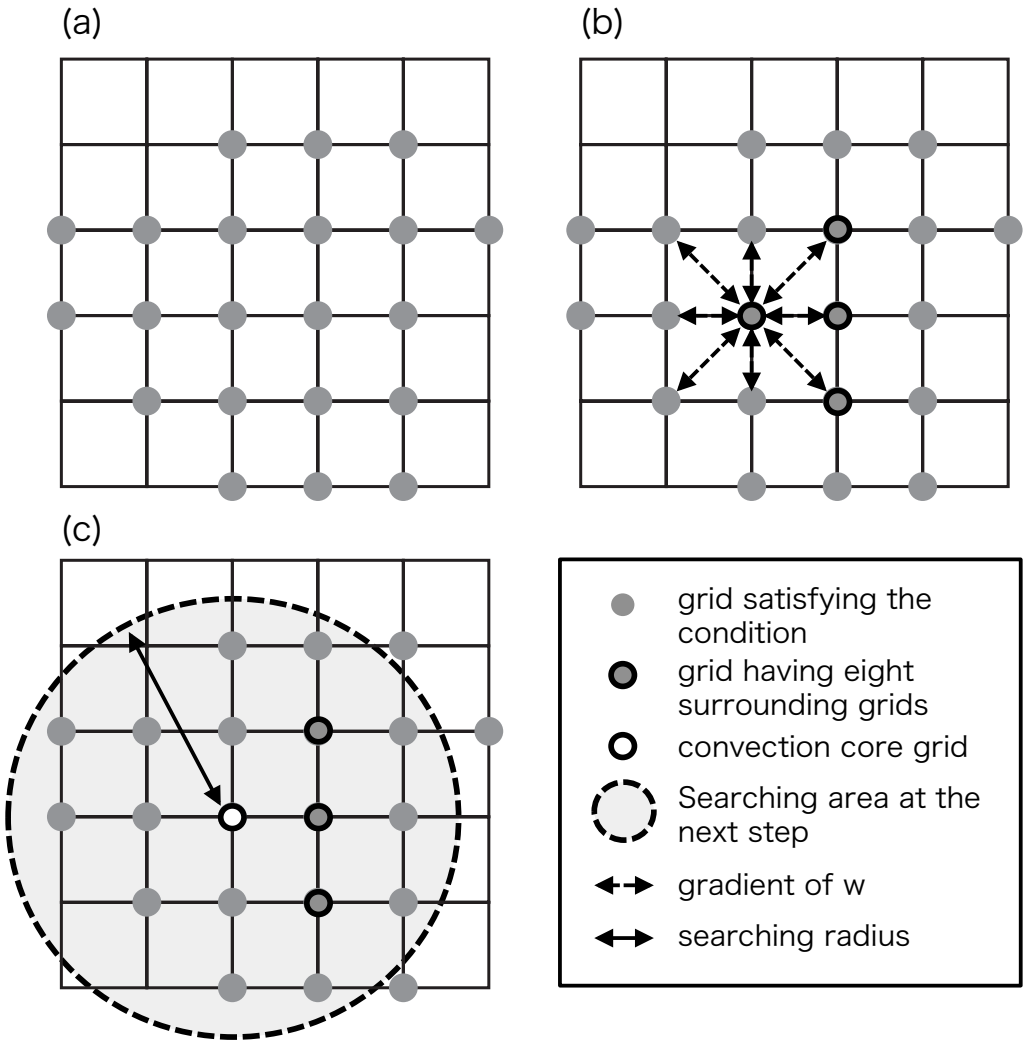

Figure 2: Schematic of the convection detecting method in the horizontal space. The gray points are the grid points satisfying all the conditions of convective grid points. The gray points surrounded by the black line are the grid points at which the surrounding 8 grid points also satisfy the convective–grid conditions. The white points with the black line indicates the convection core grid points. The light–gray circle centered at the convection–core grid point represents the area in which the convection–core grid points will be searched at the next step. The dashed arrow indicates the horizontal gradient of the vertically averaged vertical velocity.

time step. Otherwise the lifetime is 0; all the convection cores initially have a lifetime of 0 when they are first detected. The vertical layer of $C001_{t_a}$ is updated to the value at $t = t_a$ from that at $t = t_a - \Delta t$. When $C001_{t_a}$ is not a survivor of a core $t = t_a - \Delta t$

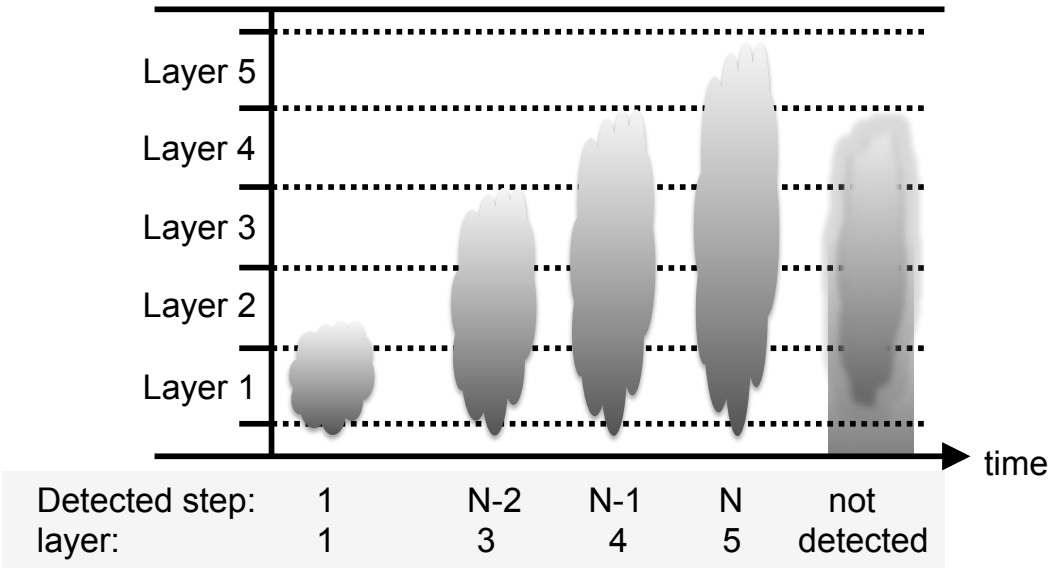

Figure 3: Schematic of the convection detecting method for the time–height section. The abscissa and ordinate are time and height, respectively. The bottom shows the time step and layer at each life stage.

(when it is first detected at $t = t_a$), the layer of $C001_{t_a}$ is set to 1 (all new convection cores form in the lower–most layer). By completing this series of tests for all the detected convection core grid points at all time steps, we obtain samples of temporally connected convection cores (i.e., the lifecycle of convection). The convection samples contain the following information:

- horizontal grid points,
- vertical layer, and
- time

at each time step in the sample ' s lifetime.

Finally, we define a full convection lifecycle to be a convection sample that satisfies the following conditions:

4. the vertical layer reaches $Nz = 5$ at the final time step, and
5. the total lifetime (over all steps) is equal to or longer than $Nz \times \Delta t$ s.

We record the following information for each instance of detected convection at each time step:

- horizontal grid points
- vertical layer
- time
- longitude and latitude
- land surface information (land/ocean)
- maximum vertical velocity w_{max} at the convection core grid point
- height of w_{max}
- combined average of the vertical velocity inside and below the layer
- combined average of the longitudinal and latitudinal velocity inside and below the layer
- combined average of the mixing ratio of hydrometeors inside and below the layer
- vertically averaged mass divergence below the 500–m level
- precipitation
- Convective Available Potential Energy (CAPE)
- Convective Inhibition (CIN)
- Lifted Condensation Level (LCL).

2.2.1 Horizontal motion

The present method for detecting the convection lifecycle determines whether convection is still present in the time step following the initial detection. For accurate detection, we must consider the horizontal motion due to convection during a time step Δt. For a constant velocity V_c over a time step, the distance moved can be written as $V_c \Delta t$. The velocity of convection is typically of the same order as the horizontal velocity in the troposphere, so $V_c = O(10 \text{ m s}^{-1})$. Therefore, after a time step Δt, if there is a convection core grid point within a radius $V_c \Delta t$ of a convection core detected in the previous timestep, that convection core is diagnosed as a survivor of the one from the previous step. Note that if the search distance is too large, this could result in the mis-detection of other,

unrelated convection cores; However, if the search distance is too small, a quickly moving convection core could be missed.

As an example, we can consider a data set with a grid spacing of 1000 m and a time step Δt of 60 s. If we consider a search radius of 2000 m, this corresponds to allowing a convection core to move two grid points ($Nx = 2$) from t_a to $t_a + \Delta t$. This corresponds to an average speed over one time step of 33.33 m s^{-1}. Note here that a speed of 33.33 m s^{-1} is very fast, but not unrealistic. It appears, however, that most convective cells do not move even one grid point (1000 m) in $\Delta t = 60$ s. This argument would be different depending on the resolution of the data, so the horizontal search for convection cores must be optimized for various cases. Here we have several options.

a) search for grid points within a specified distance

This option is to simply search for grid points within a given distance (Nx) from the grid point at which the convection core is present at $t = t_a$ without taking the search direction into consideration. Hence, the search sequence only depends on the specified search distance.

b) search grid points after adding a background velocity

Because the convection cell is expected to move at the background velocity, V_c, of the vertical level where the convection is present, this option is to conduct the search after the convection core grid point is moved by the distance it is expected to travel. In particular, the convection is assumed to move a distance $V_c \Delta t$ during a time step, and then the grid points located within a specified distance of the newly defined (moved) convection core grid point are searched. This option appears to be powerful, especially when the horizontal wind speeds are large. However, it is not certain that this option always yields better results than option a), because it is not always clear which level plays a dominant role in moving the convection core.

c) search from nearby grid points at the present time ($t = t_a$)

This option changes the sequence of the search. First, the convection core grid point at $t = t_a$ is searched, then the grid points directly adjacent to the core grid point are searched, and finally the grid points within two grid points of the core grid point are examined. This option is useful when the probability of a convection core existing after a time step is highest at the grid point location from $t = t_a$ and decreases with increasing distance from this grid point.

2.2.2 Vertical development

As discussed earlier, we divide the troposphere into Nz layers (cf. Fig. **??**); as shown above, when $Nz = 5$ the depth of each layer is a few kilometers. To meet our definition of convection, the convection core needs to start from Layer 1 and go through all layers

up to Layer 5. Here we discuss why convection must sequentially progress through the layers one by one.

The maximum vertical velocity that an air parcel can obtain (i.e., potential vertical velocity) is derived from the non-diffusive vertical momentum equation,

$$\frac{dw}{dt} = \frac{T_p - T_e}{T_e} g = B, \tag{1}$$

where T_p, T_e, and g are the temperature of the parcel, the environmental temperature, and the gravitational acceleration, respectively. We note that the vertical motion is accelerated only by buoyancy in this system. We now introduce the convective available potential energy (CAPE), which is the vertically integrated buoyant energy of an air parcel. This is defined as

$$\text{CAPE} \equiv \int_{\text{LFC}}^{\text{EL}} B dz, \tag{2}$$

where LFC and EL represent the level of free convection and the equivalent level at which the buoyancy is zero, respectively. If one assumes that all CAPE is converted to kinetic energy, the potential vertical velocity w_{maxp} is obtained:

$$w_{maxp} \approx (2\text{CAPE})^{\frac{1}{2}}. \tag{3}$$

For example, when CAPE is 800 J kg^{-1} (a typical value), w_{maxp} is 40 m s^{-1}. However, the true vertical velocity is rarely observed to reach w_{maxp}; this implies that it is rare for the entire CAPE to be consumed, which is mainly due to the presence of diffusion. Note, however, that vertical velocities larger than 30 m s^{-1} are observed in the tropics.

If we assume that the maximum vertical velocity in a numerical model is 30 m s^{-1}, it takes 100 s (= 3000 m / 30 m s^{-1}) to rise by one layer in the strongest convection. Because the timestep for the data used here is 60 s, it is rare for the peak altitude to skip a layer (i.e., move two layers) in a single time step; thus we apply the condition that convection must proceed through the atmosphere layer by layer.

3 Results

We analyze the data of Miyamoto et al. (2013, 2015, 2016) and Kajikawa et al. (2016), which consists of output from global model simulations with 870 m grid spacing in the horizontal direction, 94 layers in the vertical direction (up to 30 km in altitude), and a one-minute output interval. Due to the huge computational cost of global analysis, here we only focus on the West Pacific region with lon $\times$ lat = [0,9] $\times$ [200,270]; global results can be found in Miyamoto et al. (2013, 2015, 2016) and Kajikawa et al. (2016).

3.1 Threshold of vertically averaged mixing ratio of hydrometeors

One of the benefits of the method presented in this work is that it requires fewer specified thresholds, so it can be applied to data sets in which the atmospheric conditions vary in space or time (such as data sets covering the entire globe). The only threshold that explicitly needs to be set for our present analysis is the vertically averaged hydrometeors q_t; we set the threshold of q_t to be 0.2 g kg^{-1}. The vertically averaged vertical velocity also has a threshold value, which is 0.0 m s^{-1}, as shown earlier. However, this is obviously required to detect convection and should not be changed greatly; thresholds less than 0 would cause especially severe errors.

To examine the sensitivity of our method to the assumed threshold of averaged q_t, we tested our method using a threshold of 0.0 g kg^{-1}. Figure **??** shows histograms of q_t at the convection core grid points detected by applying that threshold. The number of convection cores having q_t in the range 0.0 – 0.1 g kg^{-1} is two orders of magnitude larger than in any other range and the number decreases exponentially with the mixing ratio. This simply indicates that more convection cores can be obtained when the threshold is smaller. The average convection structure obtained using the 0.0 g kg^{-1} threshold is, however, unlike either the observationally obtained structure or the structures obtained using the 0.2 g kg^{-1} threshold. Thus, a low threshold for q_t is desired in terms of detecting a large number of convection cores, but a non–zero threshold is needed to obtain realistic convection structures. The present method applies a threshold of 0.2 g kg^{-1}.

3.2 Vertical profiles of quantities at convection core grid points

In our detection method, we require that convection cores traverse all the layers of the atmosphere during its lifetime; this enables us to extract a reasonable lifecycle for the convection from discretized data. To verify the method, it is necessary to examine vertical profiles of physical quantities related to convection, such as the vertical velocity or mixing ratio of hydrometeors at the convection core grid points.

Figures **??** and **??** show composite vertical distributions of the vertical velocity and the hydrometeor mixing ratio of the convection cores detected in each layer; the originally defined altitudes of each layer are also indicated at the right boundary of each panel. The distributions of vertical velocity and hydrometeor mixing ratio both have a single peak which increases as the layer increases. The peak altitudes of vertical velocity correspond well with the originally defined layers, with some exceptions (Layer 2 and 5). In particular, the composite vertical velocity profile detected in Layer 5 has its peak at the altitude of Layer 4. This does not represent an error of calculation, however, because the method

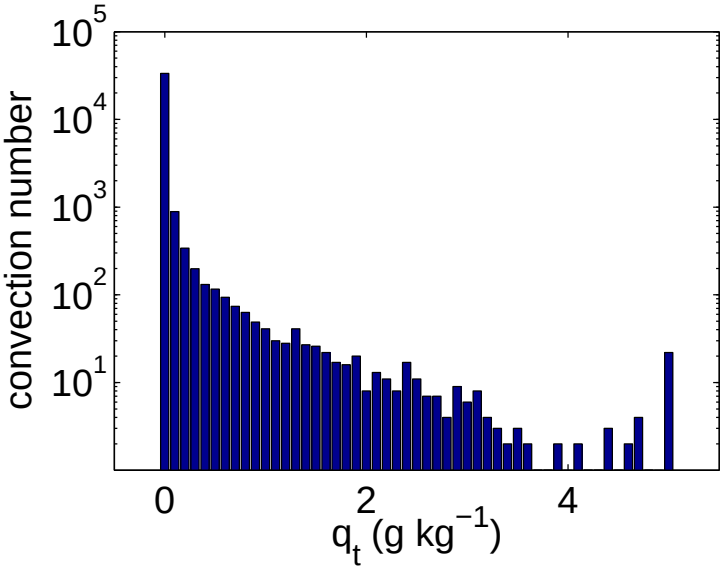

Figure 4: Histogram of q_t of the detected convection in the western north Pacific when the threshold of q_t is 0.0 g kg^{-1}. The bin is 0.5 g kg^{-1}.

does not require the convective cells to have a peak at the defined altitudes. Overall, our results indicate that the method properly detects the layer of convection height. We also find that the peak hydrometeor mixing ratio appears at lower altitudes than that of the peak vertical velocity.

4 Discussion and concluding remarks

We developed a simple methodology for detecting deep moist convection in a discretized data set. Our method requires fewer thresholds and can thus be applied to data in which the atmospheric conditions vary widely in space and time. Applying this method to a global data set with very high spatiotemporal resolution, we found that the method reasonably detects the convection lifecycle.

The proposed method is optimized for data in which the convection core is resolved by a single grid point. Because the method detects the convection core at one timestep and tracks the core in time, the core grid point needs to be clearly distinguishable from other grid points. Miyamoto et al. (2013) showed that once the horizontal grid spacing is smaller than 3.5 km, convection cores are represented by multiple grid points rather than

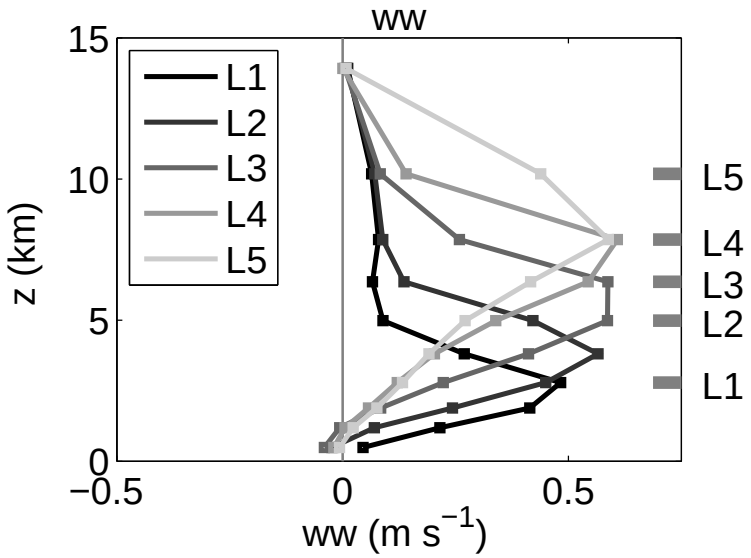

Figure 5: Vertical profiles of composited vertical velocity of convection samples detected at each layer. The bold gray lines at the right edge of panel indicate the height of original definition in the method.

a single one. This implies that our method can reasonably be applied to data with a grid spacing of a few kilometers.

There are some difficulties in applying our method to very high-resolution data, such as large-eddy simulations with resolutions of the order of 100 m. This is because the convection core location can significantly vary in time. This difficulty could be removed for certain ranges by decreasing the time interval of the output data. This does not, however, assure that there will be only a single core in the convection, and there is a possibility of multiple updraft cores. Therefore, for such a high-resolution data, the method is most likely to properly work after a spatial filter on convection distance scales is applied to smooth the data.

Acknowledgement

The numerical calculations for the analyses in this report have been conducted on the K computer.

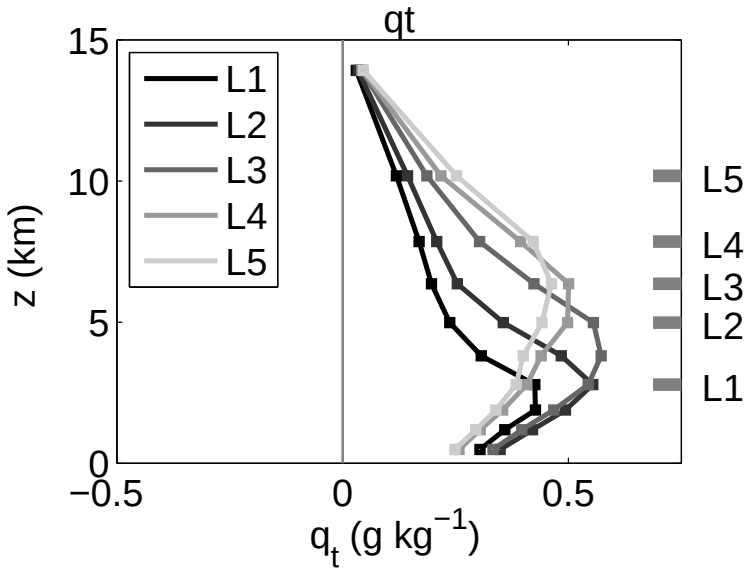

Figure 6: Same as Fig. **??**, but for composited mixing ratio of hydrometeors.

References

Bjerknes, J., 1938: Saturated-adiabatic ascent of air through dry-adiabatically descending environment, *Quart. J. Roy. Meteor. Soc.*, **64**, 325–330.

Byers, H. R., and R. R. Braham, 1948: Thunderstorm structure and circulation, *J. Meteor*, **5**, 71–86.

Dawe, J. T., and P. H. Austin, 2012: Statistical analysis of an LES shallow cumulus cloud ensemble using a cloud tracking algorithm, *Atmos. Chem. Phys.*, **12**, 1101–1119,.

Dawe, J. T., and P. H. Austin, 2013: Direct entrainment and detrainment rate distributions of individual shallow cumulus clouds in an LES, *Atmos. Chem. Phys.*, **13**, 7795–7811.

Emanuel, K. A., 1994: Atmospheric Convection, 580 pp., *Oxford University Press*, New York.

Houze, R. A., Jr., 1993: Cloud Dynamics, 573 pp., *Academic Press*, San Diego.

Kajikawa, Y., Y. Miyamoto, R. Yoshida, T. Yamaura, H. Yashiro, and H. Tomita, 2016: Resolution dependence of deep convections in a global simulation from over 10–

kilometer to sub–kilometer grid spacing, *Progress in Earth and Planetary Science*, **3**:16.

Lemone, M. A., G. M. Barnes, and E. J. Zipser, 1984: Momentum Flux by Lines of Cumulonimbus over the Tropical Oceans, *J. Atmos. Sci.*, **41**, 1914–1932.

Manabe, S., and R. T. Wetherald, 1964: Thermal Equilibrium of the Atmosphere with a Convective Adjustment, *J. Atmos. Sci.*, **21**, 361–385.

Manabe, S., and R. T. Wetherald, 1967: Thermal Equilibrium of the Atmosphere with a Given Distribution of Relative Humidity, *J. Atmos. Sci.*, **24**, 241–259.

Miyamoto, Y., Y. Kajikawa, R. Yoshida, T. Yamaura, H. Yashiro, and H. Tomita, 2013: Deep moist atmospheric convection in a sub-kilometer global simulation, *Geophys. Res. Lett.*, **40**, 4922–4926.

Miyamoto, Y, R. Yoshida, T. Yamaura, H. Yashiro, H. Tomita, and Y. Kajikawa, 2015: Does convection vary in different cloudy disturbances?, *Atmos. Sci. Lett.*, doi: 10.1002/asl2.558.

Miyamoto, Y, R. Yoshida, T. Yamaura, H. Yashiro, H. Tomita, and Y. Kajikawa, 2016: Precursors of deep moist convection in a subkilometer global simulation, *under review*

Plant, R. S., 2009: Statistical properties of cloud lifecycles in cloud-resolving models. *Atmos. Chem. Phys.*, **9**, 2195–2205.

Tung, W.-W., and M. Yanai, 2002a: Convective Momentum Transport Observed during the TOGA COARE IOP. Part I: General Features, *J. Atmos. Sci.*, **59**, 1857–1871.

Tung, W.-W., and M. Yanai, 2002b: Convective Momentum Transport Observed during the TOGA COARE IOP. Part II: Case Studies, *J. Atmos. Sci.*, **59**, 2535–2549.